Lasers in Manufacturing Conference 2015

Effect of process conditions on mechanical behavior of aluminium wrought alloy EN AW-2618 additively manufactured by Laser Beam Melting in powder bed

Michael Karg[a,d,e]*, Bhrigu Ahuja[a,d,e], Adam Schaub[b,e], Jochen Schmidt[c,e], Marius Sachs[c,e], Alexander Mahr[a], Sebastian Wiesenmayer[a], Leon Wigner[a], Karl-Ernst Wirth[c,e], Wolfgang Peukert[c,d,e], Marion Merklein[b,d,e], Michael Schmidt[a,d,e]

[a]*Institute of Photonic Technologies LPT, Friedrich-Alexander-Universität Erlangen-Nürnberg, Germany*
[b]*Institute of Manufacturing Technology LFT, Friedrich-Alexander-Universität Erlangen-Nürnberg, Germany*
[c]*Institute of Particle Technology LFG, Friedrich-Alexander-Universität Erlangen-Nürnberg, Germany*
[d]*Erlangen Graduate School in Advanced Optical Technologies SAOT, Friedrich-Alexander-Universität Erlangen-Nürnberg, Germany*
[e]*Collaorative Research Center CRC 814 "Additive Manufacturing", Friedrich-Alexander-Universität Erlangen-Nürnberg, Germany*

Abstract

Additive Manufacturing offers geometric freedom excellently suited for topology optimized light weight designs. Ideally these should be built from materials of high strength to weight ratio such as aluminium-copper wrought alloys. Yet these are considered unsuitable for welding. Today, the only class of aluminium alloys widely processed by Laser Beam Melting of Metals in powder bed (LBM) is that of aluminium-silicon cast alloys which are easily weldable. We present mechanical characteristics of LBM aluminium alloy EN AW-2618. We analyzed the chemical constitution of powder and LBM samples. We conducted tensile tests under variation of load direction relative to build-up direction. We tested samples as built and after T6 heat treatment (solution annealing, quenching and artificial aging). We found pronounced anisotropy both in the as built as well as in the T6 state. Remarkably, elongation at break of T6 samples pulled in build-up direction exceeds values from literature for conventionally manufactured EN AW-2618. For interpretation we consider boundary conditions of sample production, metallographic microsections and fracture surfaces.

Keywords: Additive Manufacturing; high-strength Aluminium Copper Wrought Alloy EN AW-2618; AlCuMgNi; 3.1924; Selective Laser Melting™; LaserCUSING™; Direct Metal-Laser-Sintering™

* Corresponding author. Tel.:+49-9131-8564101; fax: +40-9131-8523234.
E-mail address: michael.karg@lpt.uni-erlangen.de.

1. Motivation

The additive manufacturing technology of Laser Beam Melting in Powder Bed (LBM) is also known with slight variations under the registered trademarks of Selective Laser Melting™ SLM™, Direct Metal-Laser-Sintering® DMLS® or LaserCUSING™, each property of the respective owners. Industrial use of LBM has been increasing rapidly over the last years. Established fields of application include functional prototyping as well as small series production. Another field of LBM application with potentially high economic impact is beginning to be commercially developed: the manufacture of light weight components. A famous example is the LBM injection nozzle by General Electric Company, 2014. The layer-by-layer build-up inherent to LBM unlocks unmatched geometrical flexibility. This makes LBM especially suitable for realizing topology optimized designs with shapes that are optimized on a specific function or mechanical load case. Such designs typically include undercuts and can often only be manufactured conventionally after severe adaptations. Compromising optimal geometry to comply with the restrictions of production technologies reduces the added value in weight savings. The geometric flexibility of LBM can also be used to produce integral designs which would otherwise have to be assembled from multiple pieces. All joining seams are zones of potential mechanical weakness and therefore safety factors must be used. Hence, they increase total weight. Integral designs also save weight by eliminating the need for special geometry elements for joining, such as flanges.

Light weight by design can be complemented by light-weight materials. Those need to reach the mechanical properties required with a minimum of weight. For structural mechanical applications, high yield strength, tensile strength and elongation at break are examples of such desirable properties. Age-hardenable aluminium-copper alloys form a class of engineering materials which has been continuously popular for light-weight applications ever since their discovery in 1901 as described by Hornbogen, 2001. However, to the knowledge of the authors those alloys have not been researched for use in LBM by others, yet – compare Karg et al., 2014 and Ahuja et al., 2014. This can be explained by the common rating of such alloys as being unweldable and LBM physically being closely related to laser beam welding. Instead, almost exclusively aluminium-silicon alloys are popular in LBM research and industrial use. The most widely spread aluminium alloy in LBM is AlSi10Mg, compare Buchbinder, 2010, et al., 2011 and 2013 or Kempen et al., 2012. An alternative class of high-performance aluminium alloys that has been under continued scientific investigation as by Buchbinder, 2010 and Schmidtke et al., 2011 is that of Aluminium-Magnesium-Scandium alloys. Their adoption might be impeded by highly priced and not so widely available alloy components.

AW-2618 is an aluminium alloy that offers especially high performance under elevated temperatures as described by Khalil, 2014.

The goal of this contribution is to investigate the mechanical properties of AW-2618 manufactured by LBM under consideration of heat treatment and load direction relative to build-up direction.

2. Materials and Methods

2.1. Powder material

The AW-2618 powder had been argon atomized by TLS Technik GmbH. The used particle size fraction was sieved under argon atmosphere on a Haver Böcker EML 200 digital plus vibration sieve between 20 µm and 63 µm mesh width. The scanning electron microscope (SEM) picture in Fig. 1 shows a considerable amount of smaller particles remaining after sieving.

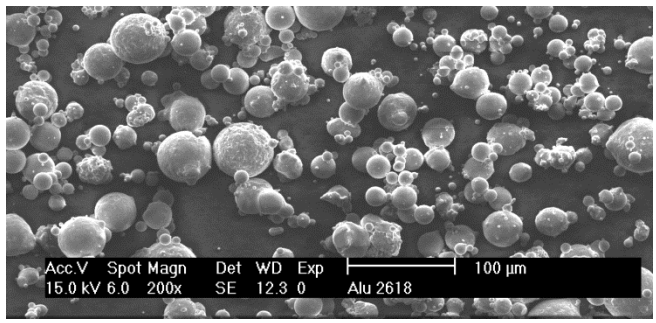

Fig. 1. SEM picture of sieved powder

2.2. Analysis of chemical elements

To check the elemental constitution of the used alloy, firstly powder and secondly a solid sample built by LBM are analyzed. This is performed by inductively coupled optical emission spectroscopy (ICP-OES) with an Optima 8300 device from Perkin Elmer at the Institute of Particle Technology (LFG).

2.3. Sample geometry and orientation

The geometry of tensile specimens is chosen according to best practice and experience at the Institute of Manufacturing Technology LFT. They are rotationally symmetrical and 64 mm long. In the clamping area the diameter is 5 mm, the testing area in the middle is 4 mm in diameter and 8 mm long, connected by a radius of 4 mm to the clamping area. A drawing is shown in Fig. 2.

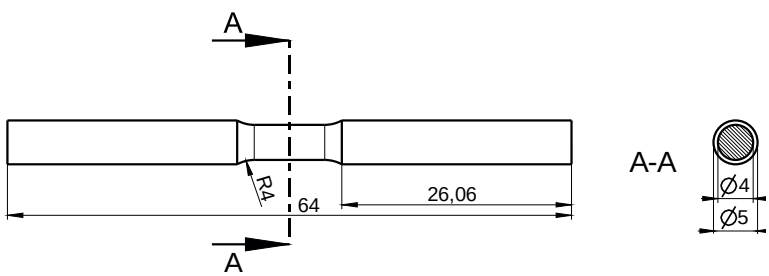

Fig. 2. tensile specimen geometry testing area 8 mm long and 4 mm diameter, all dimensions in mm

2.4. Laser beam melting on the machine ReaLizer SLM 50

The tested specimens were built on an SLM 50 LBM machine from ReaLizer GmbH. It features a custom extended z-axis and build chamber which allows vertical build height up to 90 mm instead of 40 mm standard, so vertical tensile specimens fit inside. It incorporates an Yb:YAG fiber laser from IPG Photonics Corp. with 1070 nm wavelength and maximum output power of 100 W in continuous wave mode. However, the established laser power for industrial LBM of aluminium alloys is 400 W; research with 1000 kW has been published by Buchbinder, 2011. Argon gas is circulated in the build chamber and passed through a particle filter. We used platforms cut from AlMg3 sheets for cost effectiveness. These were blasted prior to LBM, because the rough surface enables more homogeneous coating of the first powder layer and better

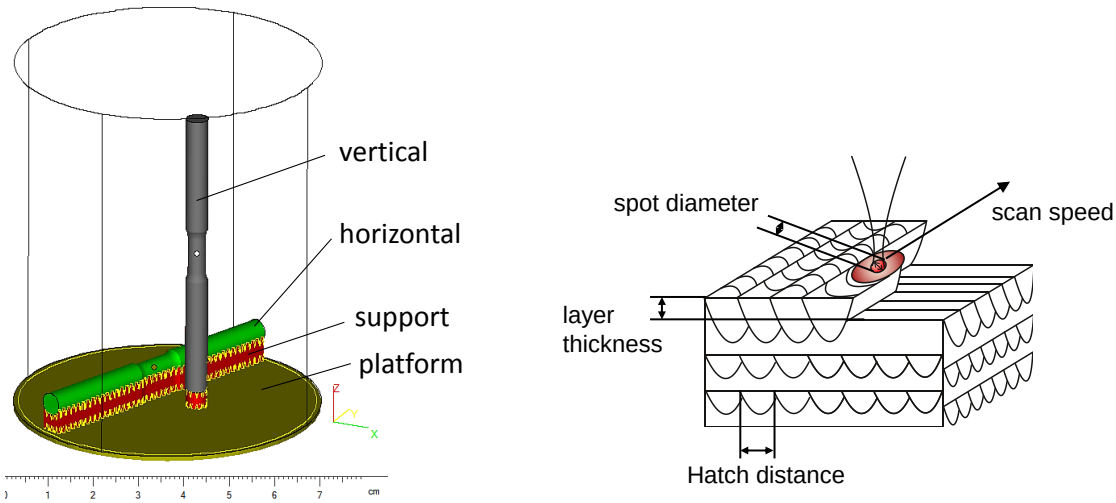

Fig. 3. left: orientation of tensile specimens in build chamber of LBM machine; right: LBM process parameters

welding connection of the supports. We used constant LBM parameters for all samples discussed in this contribution. We had optimized those for relative densities above 99.9 % using cubes of 5 mm edge length as samples, as published by Ahuja et al., 2014. In detail those LBM parameters include 200 °C build platform heating, 30 µm layer thickness and 90 µm hatch distance, as illustrated in Fig. 3.

Alternating hatch strategy was used, meaning the scanning direction was rotated by 90 ° from each layer to the next one. The scan mirror control of SLM 50 allows only indirect setting of scan speed through point distance and exposure time. We put them to 5 µm and 60 µs respectively. We had measured the actual scan speed of the laser spot on the powder bed using a high speed camera Vision Research Phantom V1210 to be approximately 112.3 mm/s. The laser spot diameter is set to 65 µm, which was measured using a PRIMES MicroSpotMonitor. The laser power was set constantly to 95 W, to avoid the numerous build interruptions due to safety shutdowns of the IPG fiber laser caused by laser back reflections which occurred at 100 W. For build preparation and design of the filigree support structures we used the software Materialise Magics.

The tensile samples were built in two orientations relative to the build platform. The first orientation is with their rotational axis horizontally in parallel to the build platform, the second standing vertically upright in an angle of 90 ° to the platform. The vertical ones are pulled in the direction of build-up, the horizontal ones are pulled in parallel to the LBM layers. Twelve specimens are built in total for tensile experiments with a sample size of three identical samples, two heat treatment states (T6 and as-built), and two orientations (horizontal and vertical).

2.5. Post-processing of samples

Half the samples were T6 heat treated, which means solution annealing for 15 hours at 530 °C in a Nabertherm N11/HR furnace, quenching in ice-water for repeatable temperature of 0 °C, artificial aging at 190 °C for 10 hours with subsequent air cooling. After removal from supports, all samples were shot peened with glass beads in an IEPCO Peenmatic 550 blasting cabin.

2.6. Metallography and fractography

For metallographic analysis, samples of cubes and broken tensile specimens were embedded in epoxy resin, grinded and polished with subsequently finer grain. For microstructure analysis, we used Bohner' s etchant. We imaged fracture surfaces of tensile specimens using reflected light microscopy and SEM.

2.7. Mechanical characterization

Tensile testing was conducted at the Institute of Manufacturing Technology LFT on a universal testing machine Z100 from Zwick/Roell. The rate of stress increase was 20 MPa/s. Vickers micro-hardness was measured with a Fischerscope H100VP. A force of 500 mN was built up over a ramp during 20 s, held stable for 5 s and released again over 20 s. Nine indentations were made per polished cube with 2 mm distance between them to avoid mutual influence, four cubes were tested first as-built and after T6 heat treatment.

3. Results and discussion

3.1. Analysis of chemical elements

The composition of chemical elements in powder before processing and an LBM built sample according to ICP-OES measurements is shown in detail in table 1 below. It shows slight deviations from the expected percentages according to the EN standard, which are highlighted in bold fonts. It is not clear what might be the reasons. Where the standard does not give a range, the single value is the maximum allowed content.

Table 1. Chemical constitution in weight-%, measured before and after LBM compared to standard DIN EN 573-3, 2009

	Cu	Mg	Fe	Ni	Mn	Si	Zn	Ti
EN AW-2618	1.8-2.7	1.2-1.8	0.9-1.4	0.8-1.4	0.25	0.15-0.25	0.15	0.2
Powder	**3.14**	1.45	1.14	1.38	-	0.16	0.06	**0.22**
Std. dev.	0.03	0.02	0.02	0.03	-	0.00	0.00	0.00
LBM sample	**3.52**	1.66	1.23	**1.54**	-	**0.29**	**0.17**	**0.23**
Std. dev.	0.03	0.02	0.02	0.03	-	0.01	0.00	0.00

3.2. Metallography

Polished cross sections show much higher porosity in horizontal samples compared to vertical ones. This is the case with all samples, as-built and T6. Fig. 4 gives an illustration in the left and middle picture. Most voids have irregular shapes. This indicates they were not caused by gas bubbles but rather by incomplete melting or poor connection of weld tracks. An approach to explain this can be that the relatively low laser power of 100 W results in a higher sensitivity of the LBM process against different thermo-dynamic boundary conditions such as they are provided by the two sample orientations. Surrounding loose powder can approximately be described as a thermal insulator, so the majority of the heat input from the laser beam must dissipate through already solidified material below into the platform towards the frame of the LBM machine. Horizontal samples might qualitatively be described as a parallel connection of resistances to the heat conduction. In comparison, vertical tensile specimens with their smaller cross section area parallel to the platform and their larger Z-height might be described as serial connection of resistances to the heat conduction. The used LBM parameters had been optimized using cubic samples of 5 mm edge length, which

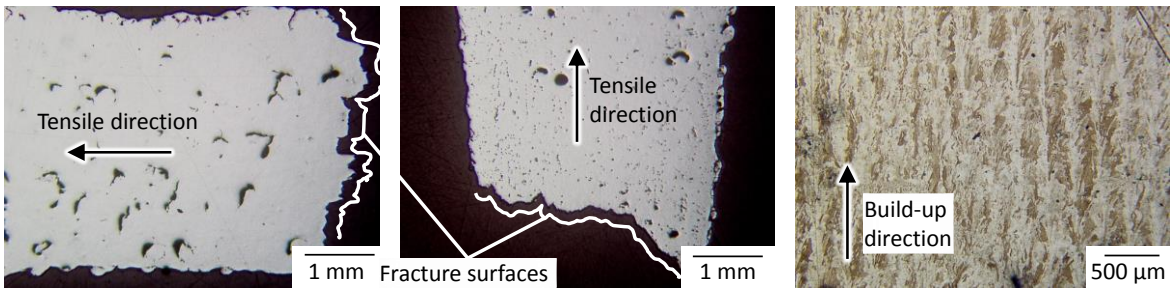

Fig. 4. broken tensile specimens in cross section, left: as-built horizontal; middle: T6 vertical; right: columnar grains in etched T6 vertical

more closely resemble the thermo-dynamic boundaries of vertical samples. Maybe these LBM parameters are not robust enough to compensate for higher heat abduction rates caused by the geometry of horizontal tensile specimens with the result of more welding defects.

All samples exhibit a pronounced directional grain growth parallel to the build-up direction, which is equivalent to the vertical z-axis of the LBM machine. An obvious reason for this seems to be the direction of the main temperature gradient during solidification of the melt. Even after T6 heat treatment, these columnar grains can be seen in etched microsections such as shown on the right of Fig. 4. Apart from voids, the microstructure of vertical samples appears overall more homogeneous than of horizontal ones.

3.3. Fractography

The fracture surfaces of vertically built specimens seem much more homogeneous then of horizontally built ones. The horizontal ones show signs of brittle fracture with separation planes – however irregular shaped- approximately orthogonal to the pulling direction and no apparent necking of the samples. Many crescent-shaped defects are visible, as shown in Fig. 5. These vary in size from about 50 µm to 200 µm and persist through T6 treatment. Their size and rounded shape indicates an origin from drop-like melt formations that did not sufficiently connect with the subjacent material. Considering the pulling direction being parallel to the LBM layers, it seems plausible that these crescents are the outlines of melt tracks. The SEM picture on the right of Fig. 5 shows spherical structures highlighted in white circles. These might be some of the smaller powder particles that had not been molten, considering the particle size distribution illustrated in Fig. 1. Terrace-like, sharp-edged breaking surfaces indicate this crescent-shaped defect might have initiated a crack with subsequent brittle fracture.

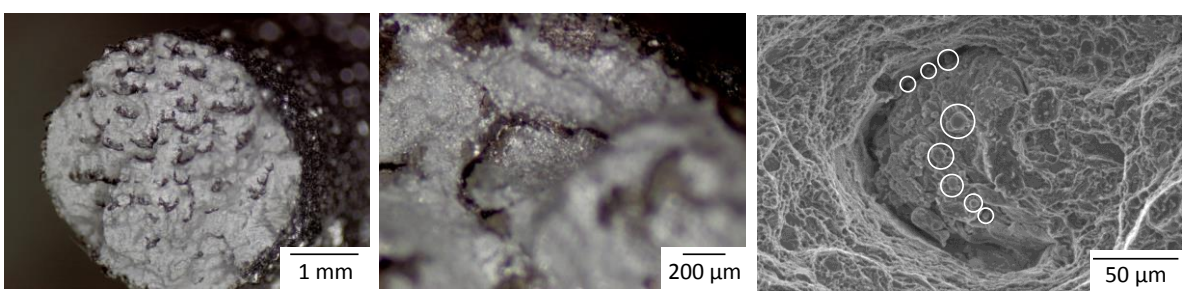

Fig. 5. fracture surfaces of horizontal samples; left: as built, middle: T6, right: T6 in SEM

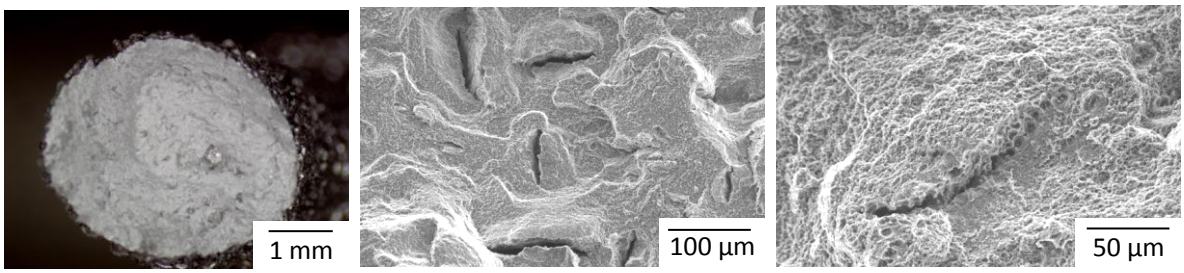

Fig. 6. fracture surfaces of vertical samples: left T6, middle SEM as-built, right SEM T6

The vertical samples show more signs of mixed fracture mode with brittle and ductile features, the latter increasing after T6 treatment. The separation plane is more inclined, the samples show some necking and the fracture surface is less irregular, as visible in Fig. 6. Opposed to the crescent-like shapes in the horizontal samples, there are noticeable straight defects in the vertical samples which are orthogonal to each other, like the alternating laser scanning pattern is in top view. These are shown in the middle of Fig. 6. The larger magnification on the right of Fig. 6. shows a fibrous, honey-comb-like surface structure indicating a more ductile fracture mode. The defect in the center seems to have formed as a connection between small dot-like inclusions that appear aligned like pearls on a necklace. In As-built condition, the surroundings of these straight defects appear more edgy; less ductile deformation seems to have happened than in T6.

3.4. Mechanical characterization

The average hardness as-built was measured on four cubic samples with nine indentations each to be approximately 120 HV, the standard deviation was around 10 HV. T6 heat treatment led to an increase of 40 HV to an average of 160 HV with a similar standard deviation of roughly 10 HV. Literature values for comparison with conventionally manufactured AW-2618 T6 from Hesse, 2012 and Matweb, 2015 are considerably lower with 130 HV. Vickers hardness of the state-of-the-art LBM aluminium cast alloy AlSi10Mg (equivalent to EN AC-43000) was determined by Buchbinder, 2011 to be between 140 HV and 150 HV as-built and by Buchbinder, 2013 to be between 80 HV and 120 HV after T6 heat treatment.

Yield strength, tensile strength and elongation at break obtained from tensile tests are compared in Fig. 7. Except elongation at break of the horizontal samples, all the other characteristic values benefit from T6 heat treatment compared to the as-built state. Most remarkably, the elongation at break of the T6 vertical samples is more than 2.5 times as high as that of conventionally processed AW-2618. The as-built vertical samples achieve consistently higher elongation at break. Yield strength of all samples is far below values for conventionally manufactured AW-2618 from Hesse, 2012. The same is the case with the tensile strength; with 400 MPa the T6 vertical samples do reach 90 % of the literature value, however. With the exception of yield strength, all characteristics seem to be highly anisotropic. Considering the higher porosity and larger defect size in the horizontal samples discussed above, this seems to be self-evident. However it seems surprising that the yield strength of the as-built vertical samples is even lower than of the as-built horizontal ones. Regarding the very different quality of horizontal and vertical samples, it seems not to be justified to discuss potential effects of the columnar grain structure. The same is considered for potential overaging effects of the platform heating temperature as described by Khalil, 2014. It exceeds the temperature used for artificial aging. LBM samples are subject to this environment for the duration of the whole LBM job. The build jobs conducted for this contribution lasted up to 25 hours. Additional error sources must be taken into account when interpreting these test results. Only three identically prepared

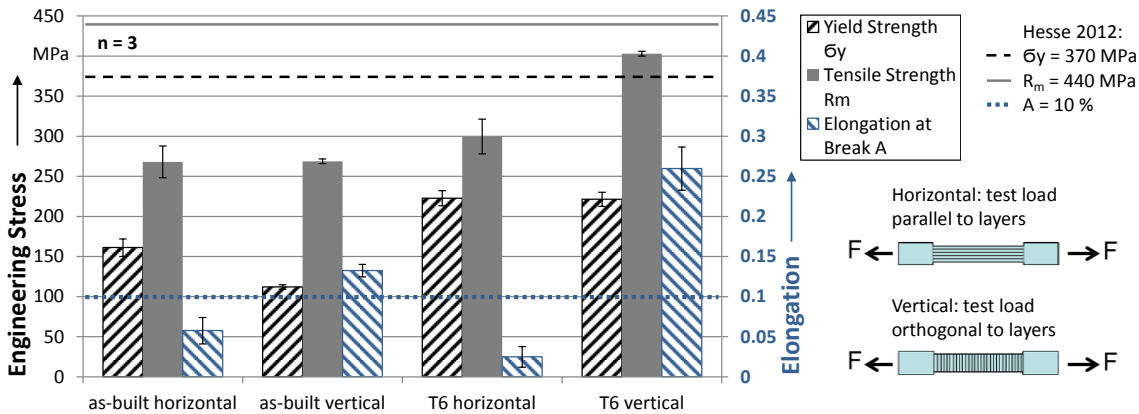

Fig. 7. tensile testing results depending on heat treatment and build orientation compared to conventionally processed AW-2618 T6

samples of each variation have been tested – however, deviations between them are considerably small. The rough surfaces created in LBM have been smoothened by glass bead blasting. This might have led to residual compressive stresses and thus improved mechanical performance. On the other hand, the remaining roughness is still bigger than that of conventionally machined samples which should decrease performance. Rough samples might also more easily slip in the hydraulic clamping units of the testing machine. However, such slippage should result in irregularities in the stress-strain curves, e. g. exceptionally low slopes or repeated kinks. We observed no such obvious irregularities.

4. Conclusion and Outlook

The production of tensile specimens with low porosity from AW-2618 with an LBM machine of 100 W laser power is possible; however process stability seems to be sensitive to geometric boundaries. Horizontally built samples exhibit larger porosity, less homogeneous microstructure and inferior mechanical characteristics. As-built samples do not meet literature values for yield strength and tensile strength, but when loaded in build-up direction, elongation at break exceeds literature values from conventional processed T6 samples. Vertically built and T6 heat treated samples are still not competitive in yield strength, but reach 90 % of tensile strength and 250 % of the value for elongation at break given by Hesse, 2012. Columnar grains parallel to build-up direction are distinct as-built and after T6 treatment. Microhardness of as-built samples of 120 HV is similar to literature values for T6; additional T6 heat treatment of LBM samples raises it to 160 HV.

For future experiments processing AW-2618, higher available laser power might help to establish a more robust process regime, as might optimization of the scanning strategies for different geometries. Milling or turning of samples could reduce surface effects. In turn, effects of columnar grain structure and long LBM job durations might become more accessible to research. Larger numbers of tested samples would improve the power of conveyed statements.

Acknowledgements

We acknowledge the measurement of the focus diameter on the Realizer SLM 50 conducted by Aleksandr Fedorov and Oliver Hentschel, both affiliated to the Institute of Photonic Technologies LPT, with the support of Matthias Fockele of ReaLizer GmbH and Christof Schöberl of PRIMES GmbH. This research was conducted within the Collaborative Research Center CRC 814 Additive Manufacturing - "SFB 814 Additive Fertigung"- subproject A 5 "Selective Laser Melting of Composite Material Systems for the Manufacture of Metallic Light-Weight Structures" and supported by the Erlangen Graduate School in Advanced Optical Technologies (SAOT) in the framework of the German excellence initiative. Both SFB 814 and SAOT receive financial support from the German Research Foundation DFG.

References

General Electric Company, 2014. World's First Plant to Print Jet Engine Nozzles in Mass Production. Press Release July 15th 2014 http://www.gereports.com/post/ 91763815095/worlds-first-plant-to-print-jet-engine-nozzles-in-mass. Accessed May 25th 2015

Hornbogen, E., 2001. Hundred years of precipitation hardening. Journal of Light Metals 1, p. 127-132

Karg, M., Ahuja, B., Kuryntsev, S., Gorunov, A., Schmidt, M., 2014. Processability of high strength Aluminium-Copper alloys AW-2022 and 2024 by Laser Beam Melting in Powder Bed. 25th Solid Freeform Fabrication Symposium at the University of Texas in Austin (USA) 2014

Ahuja, B., Karg, M., Nagulin, K., Schmidt, M., 2014. Fabrication and Characterization of High Strength Al-Cu alloys Processed Using Laser Beam Melting in Metal Powder Bed. Physics Procedia 56, p. 135-146

Buchbinder, D., 2010. Generative Fertigung von Aluminiumbauteilen für die Serienproduktion. AluGenerativ Abschlussbericht BMBF 01RIO639A-D

Buchbinder, D., 2011. High Power Selective Laser Melting of Aluminum Parts. Physics Procedia 12, p. 271-278

Buchbinder, D., 2013. Selective Laser Melting von Aluminiumgusslegierungen. PhD Dissertation RWTH Aachen, 2013

Kempen, K., Thijs, L., Van Humbeeck, J., Kruth, J., 2012. Mechanical Properties of AlSi10Mg Produced by Selective Laser Melting. Physics Procedia 39, p. 439-446

Schmidtke, K., Palm, F., Hawkins, A., Emmelmann, C., 2011. Process and Mechanical Properties: Applicability of a Scandium modified Al-alloy for Laser Additive Manufacturing. Physics Procedia 12, p. 369–374

Khalil, O., 2014. Isothermes Kurzzeitermüdungsverhalten der hochwarmfesten Aluminium-Knetlegierung 2618a (AlCu2Mg1,5Ni), PhD Dissertation, Karlsruher Institut für Technologie (KIT)

DIN Deutsches Institut für Normung e. V. 2009. DIN EN 573-3 Aluminium und Aluminiumlegierungen - Chemische Zusammensetzung und Form von Halbzeug.

Hesse, W., 2012. Aluminium Schlüssel

Matweb: Aluminum 2618-T61; URL: http://matweb.com/search/datasheet.aspx?MatGUID=f6d0bebbfc7248838243 b7fa141431ba, last accessed on May 24th, 2015